Supplementary Material

Rapid oxidation of phenolic compounds by O_3 and $HO^{\bullet}$: effects of air-water interface and mineral dust in tropospheric chemical processes

Yanru Huo[a], Mingxue Li[b], Xueyu Wang[c], Jianfei Sun[d], Yuxin Zhou[a], Yuhui Ma[a], Maoxia He[a,*]

[a] Environment Research Institute, Shandong University, Qingdao 266237, P. R. China

[b] Department of Civil and Environmental Engineering, The Hong Kong Polytechnic University, Hong Kong SAR, China

[c] College of Geography and Environmental Sciences, Zhejiang Normal University, Jinhua 321004, China

[d] School of Environmental and Materials Engineering, Yantai University, Yantai, 264005, PR China

---

*Corresponding author: Prof. Maoxia He

Tel: 86-532-58631972 (o)

Fax: 86-532-5863 1986

E-mail address: hemaox@sdu.edu.cn

Table S1. Gibbs free energy of activation ($\Delta G^{\ddagger}$) for the O_3-initiated reaction of phe, 4-HBA, and VL. Unit: kcal mol $^{-1}$.

Compounds	C1 – C2	C2 – C3	C3 – C4	C4 – C5	C5 – C6	C6 – C1
			Gas-phase			
Ph	19.03	20.60	20.46	–	–	–
4-HBA	23.59	24.22	24.84	24.33	23.47	24.52
VL	22.54	24.46	21.00	25.95	22.51	23.22
			Bulk water			
Ph	14.94	17.88	15.75			
4-HBA	20.21	21.27	22.38	20.92	19.84	20.81
VL	19.17	20.89	17.89	24.43	18.56	19.56
			A-W interface			
Ph	15.18	18.10	12.86			
4-HBA	21.76	22.03	24.69	25.24	23.88	22.36
VL	14.15	19.16	16.01	21.41	21.02	19.81
			TiO_2 clusters			
Ph	25.34	24.46	24.30			
4-HBA	25.91	23.51	23.96	26.53	23.23	27.83
VL	15.98	11.42	17.44	11.14	13.37	14.65

Table S2. Gibbs free energy of reaction ($\Delta_r G$) for the O_3-initiated reaction of MeP and halo-parabens. Unit: kcal mol $^{-1}$.

Compounds	C1 – C2	C2 – C3	C3 – C4	C4 – C5	C5 – C6	C6 – C1
			Gas-phase			
Ph	-28.85	-25.44	-24.77			
4-HBA	-24.26	-21.71	-17.86	-16.21	-22.74	-21.46
VL	-23.72	-19.55	-20.42	-14.57	-24.02	-26.62
			Bulk water			
Ph	-31.58	-27.21	-30.11			
4-HBA	-26.18	-23.81	-20.32	-19.72	-28.56	-24.50
VL	-27.10	-23.10	-24.33	-19.54	-31.30	-31.11
			A-W interface			
Ph	-30.00	-27.30	-27.01			
4-HBA	-21.92	-25.40	-19.38	-18.69	-21.35	-23.34
VL	-31.29	-34.68	-16.62	-22.71	-30.85	-29.35
			TiO_2 clusters			
Ph	-31.22	-21.38	-19.86			
4-HBA	-17.42	-26.57	-17.96	-15.98	-24.45	-16.25
VL	-24.60	-20.40	-20.31	-16.87	-23.57	-31.74

Table S3. Gibbs free energy of activation ($\Delta G^{\ddagger}$) for the HO$^{\bullet}$-initiated reaction of phe, 4-HBA, and VL. Unit: kcal mol^{-1}.

Compounds	$R_{RAF}1$	$R_{RAF}2$	$R_{RAF}3$	$R_{RAF}4$	$R_{RAF}5$	$R_{RAF}6$	$R_{HAA}2$	$R_{HAA}3$	$R_{HAA}4$	$R_{HAA}5$	$R_{HAA}6$	$R_{HAA}7$	$R_{HAA}8$	$R_{HAA}9$
						Gas-phase								
Ph	6.37	3.45	7.59	5.57	–	–	6.86	45.19	8.56	–	–	4.08	–	–
4-HBA	10.55	7.42	10.86	10.45	11.80	10.00	10.33	11.70	–	10.30	49.33	7.61	4.87	–
VL	7.85	6.39	7.69	9.32	10.43	10.29	–	33.89	–	10.37	46.96	8.81	4.90	10.47
						Bulk water								
Ph	7.17	5.27	5.60	2.46	–	–	9.03	29.08	6.98	–	–	5.39	–	–
4-HBA	11.22	9.43	9.86	8.01	8.77	6.96	11.22	9.43	–	9.86	8.01	8.77	6.96	–
VL	6.69	6.58	7.72	7.62	6.94	7.69	–	26.74	–	10.63	30.17	10.38	6.38	9.96
						A-W interface								
Ph	6.81	-0.97	7.86	4.38	–	–	6.88	7.03	7.30	–	–	1.95	–	–
4-HBA	12.04	5.35	11.37	9.33	10.82	8.10	11.22	12.74	–	9.38	14.53	8.76	8.17	–
VL	5.24	6.48	3.25	1.67	1.10	3.48	–	10.35	–	8.95	8.89	5.43	1.21	4.60
						TiO_2 clusters								
Ph	4.70	5.14	16.98	11.50	–	–	7.47	12.16	12.48	–	–	4.89	–	–
4-HBA	12.55	8.95	11.47	2.64	12.85	10.20	11.08	8.11	–	11.50	11.45	13.46	4.99	–
VL	-1.88	-3.22	-2.78	-3.81	-0.40	0.40	–	5.78	–	1.73	2.20	-1.05	-7.48	-0.51
VL^{pre}	0.00	0.00	0.00	0.00	0.00	0.00	–	17.28	–	0.00	0.00	-0.01	12.30	0.00

VL^{pre}: $\Delta G^{\ddagger}$ values of free energy difference between transition states and reaction complexes.

Table S4. Gibbs free energy of reaction ($\Delta_r G$) for the HO•-initiated reaction of phe, 4-HBA, and VL. Unit: kcal mol $^{-1}$.

Compounds	$R_{RAF}1$	$R_{RAF}2$	$R_{RAF}3$	$R_{RAF}4$	$R_{RAF}5$	$R_{RAF}6$	$R_{HAA}2$	$R_{HAA}3$	$R_{HAA}4$	$R_{HAA}5$	$R_{HAA}6$	$R_{HAA}7$	$R_{HAA}8$	$R_{HAA}9$
						Gas-phase								
Ph	-15.85	-15.78	-11.57	-12.81	–	–	-9.92	-10.82	-9.57	–	–	-32.39	–	–
4-HBA	-12.29	-11.73	-9.12	-4.21	-7.88	-8.39	-6.31	-6.51	–	-5.67	-5.17	-27.53	-28.86	–
VL	-16.53	-13.40	-10.20	-6.06	-11.05	-7.33	–	1.66	–	-5.07	-5.26	-29.65	-29.18	-21.19
						Bulk water								
Ph	-13.36	-14.77	-16.58	-13.39	–	–	-6.92	-6.43	-6.43	–	–	-31.97		–
4-HBA	-12.38	-9.50	-9.45	-5.31	-11.28	-9.81	-7.96	-8.82	–	-9.33	-8.11	-28.25	-29.34	–
VL	-30.28	-27.25	-24.49	-6.23	-15.18	-8.18	–	-4.75	–	-8.14	-7.70	-34.53	-28.99	-22.24
						A-W interface								
Ph	-14.07	-17.70	-11.90	-14.04	–	–	-11.10	-11.77	-10.60	–	–	-31.31	–	–
4-HBA	-11.49	-10.79	-8.10	-9.68	-8.32	-10.06	-6.48	-6.39	–	-7.35	–	-24.50	-29.95	–
VL	-23.74	-7.11	-12.13	-14.08	-14.05	-17.02	–	-4.94	–	-9.06	-6.62	-32.29	-28.21	-22.58
						TiO_2 clusters								
Ph	-20.66	-15.51	-10.59	-8.04	–	–	-6.92	-6.43	-6.43	–	–	-31.97	–	–
4-HBA	-17.85	-9.27	-10.91	-2.15	-13.04	-7.96	-5.34	-6.68	–	-8.71	-3.85	-21.60	-20.82	–
VL	-29.72	-21.80	-25.06	-19.88	-25.90	-16.39	–	-29.72	–	-21.80	-25.06	-19.88	-25.90	-16.39

Table S5. The reaction rate constants (k_{uni}/cm^3 molecule^{-1} s^{-1}) for the ozonolysis of Ph, 4-HBA, and VL in different environmental media (EM) over the temperature range of 318 – 278 K.

EM	k	318	308	298	288	278	Γ
				Ph			
A-W	k_1	6.69×10^{-7}	6.33×10^{-7}	5.98×10^{-7}	5.64×10^{-7}	5.32×10^{-7}	100.00%
	k_2	2.50×10^{-17}	1.08×10^{-17}	4.46×10^{-18}	1.73×10^{-18}	6.28×10^{-19}	0.00%
	k_3	2.33×10^{-19}	8.67×10^{-20}	3.03×10^{-20}	9.85×10^{-21}	2.97×10^{-21}	0.00%
	k_{tot}	6.69×10^{-7}	6.33×10^{-7}	5.98×10^{-7}	5.64×10^{-7}	5.32×10^{-7}	100.00%
TiO_2	k_1	2.65×10^{-24}	6.82×10^{-25}	1.61×10^{-25}	3.44×10^{-26}	6.61×10^{-27}	8.73%
	k_2	1.01×10^{-23}	2.71×10^{-24}	6.69×10^{-25}	1.50×10^{-25}	3.04×10^{-26}	36.33%
	k_3	1.48×10^{-23}	4.04×10^{-24}	1.01×10^{-24}	2.31×10^{-25}	4.77×10^{-26}	54.94%
	k_{tot}	2.75×10^{-23}	7.43×10^{-24}	1.84×10^{-24}	4.16×10^{-25}	8.47×10^{-26}	100.00%
Gas phase	k_1	5.76×10^{-20}	5.82×10^{-20}	5.17×10^{-20}	4.88×10^{-20}	4.61×10^{-20}	97.94%
	k_2	4.76×10^{-21}	1.57×10^{-21}	4.79×10^{-22}	1.35×10^{-22}	3.50×10^{-23}	0.91%
	k_3	5.97×10^{-21}	1.98×10^{-21}	6.09×10^{-22}	1.72×10^{-22}	4.42×10^{-23}	1.16%
	k_{tot}	6.83×10^{-20}	6.17×10^{-20}	5.27×10^{-20}	4.91×10^{-20}	4.62×10^{-20}	100.00%
Bulk water	k_1	1.43×10^{12}	1.51×10^{12}	1.59×10^{12}	1.68×10^{12}	1.77×10^{12}	39.58%
	k_2	8.96×10^{11}	9.59×10^{11}	1.03×10^{12}	1.10×10^{12}	1.18×10^{12}	25.56%
	k_3	1.25×10^{12}	1.32×10^{12}	1.40×10^{12}	1.48×10^{12}	1.57×10^{12}	34.86%
	k_{tot}	3.58×10^{12}	3.79×10^{12}	4.02×10^{12}	4.26×10^{12}	4.51×10^{12}	100.00%
				4-HBA			
A-W	k_1	3.74×10^{-22}	1.16×10^{-22}	3.32×10^{-23}	8.76×10^{-24}	2.10×10^{-24}	48.92%
	k_2	2.44×10^{-22}	7.45×10^{-23}	2.10×10^{-23}	5.46×10^{-24}	1.29×10^{-24}	30.98%
	k_3	3.65×10^{-24}	9.73×10^{-25}	2.38×10^{-25}	5.28×10^{-26}	1.05×10^{-26}	0.35%
	k_4	1.54×10^{-24}	3.98×10^{-25}	9.42×10^{-26}	2.03×10^{-26}	3.91×10^{-27}	0.14%
	k_5	1.33×10^{-23}	3.69×10^{-24}	9.44×10^{-25}	2.20×10^{-25}	4.63×10^{-26}	1.39%
	k_6	1.48×10^{-22}	4.45×10^{-23}	1.24×10^{-23}	3.15×10^{-24}	7.31×10^{-25}	18.22%
	k_{tot}	7.85×10^{-22}	2.40×10^{-22}	6.79×10^{-23}	1.77×10^{-23}	4.18×10^{-24}	100.00%

TiO_2	k_1	5.51×10^{-25}	1.38×10^{-25}	3.16×10^{-26}	6.56×10^{-27}	1.22×10^{-27}	0.59%
	k_2	2.33×10^{-23}	6.59×10^{-24}	1.72×10^{-24}	4.08×10^{-25}	8.78×10^{-26}	32.26%
	k_3	1.14×10^{-23}	3.15×10^{-24}	8.00×10^{-25}	1.85×10^{-25}	3.87×10^{-26}	15.02%
	k_4	1.95×10^{-25}	4.73×10^{-26}	1.04×10^{-26}	2.08×10^{-27}	3.70×10^{-28}	0.20%
	k_5	3.64×10^{-23}	1.04×10^{-23}	2.76×10^{-24}	6.68×10^{-25}	1.46×10^{-25}	51.90%
	k_6	2.67×10^{-26}	6.07×10^{-27}	1.25×10^{-27}	2.32×10^{-28}	3.82×10^{-29}	0.02%
	k_{tot}	7.19×10^{-23}	2.04×10^{-23}	5.32×10^{-24}	1.27×10^{-24}	2.74×10^{-25}	100.00%
Gas phase	k_1	2.11×10^{-23}	5.96×10^{-24}	1.55×10^{-24}	3.67×10^{-25}	7.86×10^{-26}	31.36%
	k_2	7.84×10^{-24}	2.14×10^{-24}	5.37×10^{-25}	1.23×10^{-25}	2.53×10^{-26}	10.89%
	k_3	2.88×10^{-24}	7.61×10^{-25}	1.84×10^{-25}	4.06×10^{-26}	8.04×10^{-27}	3.74%
	k_4	6.46×10^{-24}	1.75×10^{-24}	4.37×10^{-25}	9.91×10^{-26}	2.03×10^{-26}	8.85%
	k_5	2.56×10^{-23}	7.27×10^{-24}	1.90×10^{-24}	4.54×10^{-25}	9.80×10^{-26}	38.50%
	k_6	4.95×10^{-24}	1.33×10^{-24}	3.29×10^{-25}	7.39×10^{-26}	1.50×10^{-26}	6.67%
	k_{tot}	6.88×10^{-23}	1.92×10^{-23}	4.93×10^{-24}	1.16×10^{-24}	2.45×10^{-25}	100.00%
Bulk water	k_1	3.10×10^{11}	3.36×10^{11}	3.64×10^{11}	3.95×10^{11}	4.28×10^{11}	18.45%
	k_2	2.61×10^{11}	2.85×10^{11}	3.10×10^{11}	3.37×10^{11}	3.67×10^{11}	15.70%
	k_3	2.15×10^{11}	2.35×10^{11}	2.57×10^{11}	2.81×10^{11}	3.08×10^{11}	13.04%
	k_4	2.74×10^{11}	2.98×10^{11}	3.24×10^{11}	3.52×10^{11}	3.82×10^{11}	16.39%
	k_5	3.28×10^{11}	3.54×10^{11}	3.83×10^{11}	4.14×10^{11}	4.47×10^{11}	19.39%
	k_6	2.84×10^{11}	3.09×10^{11}	3.36×10^{11}	3.65×10^{11}	3.97×10^{11}	17.03%
	k_{tot}	1.67×10^{12}	1.82×10^{12}	1.97×10^{12}	2.14×10^{12}	2.33×10^{12}	100.00%
				VL			
A-W	k_1	6.12×10^{-17}	2.80×10^{-17}	1.21×10^{-17}	4.99×10^{-18}	1.93×10^{-18}	95.90%
	k_2	2.26×10^{-20}	7.97×10^{-21}	2.63×10^{-21}	8.07×10^{-22}	2.28×10^{-22}	0.02%
	k_3	3.18×10^{-18}	1.32×10^{-18}	5.16×10^{-19}	1.90×10^{-19}	6.51×10^{-20}	4.07%
	k_4	6.27×10^{-22}	1.97×10^{-22}	5.74×10^{-23}	1.54×10^{-23}	3.77×10^{-24}	0.00%
	k_5	1.23×10^{-21}	3.96×10^{-22}	1.18×10^{-22}	3.27×10^{-23}	8.23×10^{-24}	0.00%
	k_6	8.00×10^{-21}	2.73×10^{-21}	8.70×10^{-22}	2.57×10^{-22}	6.95×10^{-23}	0.01%
	k_{tot}	6.44×10^{-17}	2.93×10^{-17}	1.27×10^{-17}	5.18×10^{-18}	1.99×10^{-18}	100.00%

TiO_2	k_1	3.63×10^{-18}	1.51×10^{-18}	5.97×10^{-19}	2.21×10^{-19}	7.66×10^{-20}	0.02%
	k_2	4.83×10^{-15}	2.54×10^{-15}	1.29×10^{-15}	6.22×10^{-16}	2.86×10^{-16}	38.91%
	k_3	3.51×10^{-19}	1.36×10^{-19}	4.93×10^{-20}	1.68×10^{-20}	5.28×10^{-21}	0.00%
	k_4	7.19×10^{-15}	3.83×10^{-15}	1.96×10^{-15}	9.63×10^{-16}	4.50×10^{-16}	59.44%
	k_5	2.22×10^{-16}	1.06×10^{-16}	4.82×10^{-17}	2.08×10^{-17}	8.48×10^{-18}	1.46%
	k_6	3.01×10^{-17}	1.35×10^{-17}	5.71×10^{-18}	2.29×10^{-18}	8.63×10^{-19}	0.17%
	k_{tot}	1.23×10^{-14}	6.50×10^{-15}	3.30×10^{-15}	1.61×10^{-15}	7.46×10^{-16}	100.00%
Gas-phase	k_1	1.05×10^{-22}	3.10×10^{-23}	8.51×10^{-24}	2.14×10^{-24}	4.87×10^{-25}	6.32%
	k_2	5.11×10^{-24}	1.38×10^{-24}	3.40×10^{-25}	7.63×10^{-26}	1.54×10^{-26}	0.25%
	k_3	1.19×10^{-21}	3.81×10^{-22}	1.13×10^{-22}	3.11×10^{-23}	7.82×10^{-24}	84.30%
	k_4	4.76×10^{-25}	1.19×10^{-25}	2.70×10^{-26}	5.54×10^{-27}	1.02×10^{-27}	0.02%
	k_5	1.16×10^{-22}	3.46×10^{-23}	9.54×10^{-24}	2.41×10^{-24}	5.52×10^{-25}	7.09%
	k_6	3.58×10^{-23}	1.03×10^{-23}	2.71×10^{-24}	6.55×10^{-25}	1.43×10^{-25}	2.02%
	k_{tot}	1.45×10^{-21}	4.58×10^{-22}	1.35×10^{-22}	3.64×10^{-23}	9.02×10^{-24}	100.00%
Bulk water	k_1	3.455×10^{11}	3.712×10^{11}	3.986×10^{11}	4.278×10^{11}	4.590×10^{11}	18.08%
	k_2	2.671×10^{11}	2.897×10^{11}	3.142×10^{11}	3.406×10^{11}	3.691×10^{11}	14.25%
	k_3	4.161×10^{11}	4.437×10^{11}	4.728×10^{11}	5.036×10^{11}	5.362×10^{11}	21.45%
	k_4	1.479×10^{11}	1.631×10^{11}	1.798×10^{11}	1.980×10^{11}	2.181×10^{11}	8.16%
	k_5	4.005×10^{11}	4.302×10^{11}	4.619×10^{11}	4.960×10^{11}	5.326×10^{11}	20.96%
	k_6	3.253×10^{11}	3.501×10^{11}	3.767×10^{11}	4.052×10^{11}	4.357×10^{11}	17.09%
	k_{tot}	1.90×10^{12}	2.05×10^{12}	2.20×10^{12}	2.37×10^{12}	2.55×10^{12}	100.00%

Table S6. The reaction rate constants (k_{uni}/cm^3 molecule $^{-1}$ s $^{-1}$) for the HO$^{\bullet}$-initiated reaction of Ph, 4-HBA, and VL in different environmental media (EM) over the temperature range of 318 – 278 K.

EM	k	318	308	298	288	278	Γ
				Ph-R_{RAF}			
	k_1	7.33×10^{-12}	4.90×10^{-12}	3.20×10^{-12}	2.03×10^{-12}	1.25×10^{-12}	0.00%
	k_2	2.74×10^{-6}	2.70×10^{-6}	2.67×10^{-6}	2.64×10^{-6}	2.62×10^{-6}	99.15%
	k_3	2.77×10^{-12}	1.75×10^{-12}	1.08×10^{-12}	6.44×10^{-13}	3.71×10^{-13}	0.00%
	k_4	3.27×10^{-10}	2.47×10^{-10}	1.84×10^{-10}	1.34×10^{-10}	9.59×10^{-11}	0.01%
	k_{totRAF}	2.74×10^{-6}	2.70×10^{-6}	2.67×10^{-6}	2.64×10^{-6}	2.62×10^{-6}	99.16%
A-W				Ph-R_{HAA}ben			
	k_1	2.09×10^{-11}	1.42×10^{-11}	9.43×10^{-12}	6.10×10^{-12}	3.83×10^{-12}	0.00%
	k_2	1.87×10^{-11}	1.27×10^{-11}	8.39×10^{-12}	5.40×10^{-12}	3.37×10^{-12}	0.00%
	k_3	6.47×10^{-12}	4.33×10^{-12}	2.82×10^{-12}	1.79×10^{-12}	1.10×10^{-12}	0.00%
	$k_{totHAAben}$	4.61×10^{-11}	3.12×10^{-11}	2.06×10^{-11}	1.33×10^{-11}	8.30×10^{-12}	0.00%
				Ph-R_{HAA}sub			
	k_7	2.95×10-8	2.59×10^{-8}	2.26×10^{-8}	1.96×10^{-8}	1.69×10^{-8}	0.84%
	$k_{totHAAsub}$	2.95×10^{-8}	2.59×10^{-8}	2.26×10^{-8}	1.96×10^{-8}	1.69×10^{-8}	0.84%
	k_{tot}	2.77×10^{-6}	2.73×10^{-6}	2.69×10^{-6}	2.66×10^{-6}	2.63×10^{-6}	100.00%
				Ph-R_{RAF}			
	k_1	1.71×10^{-10}	1.51×10^{-10}	1.11×10^{-10}	7.93×10^{-11}	5.57×10^{-11}	34.90%
	k_2	1.91×10^{-10}	1.38×10^{-10}	9.85×10^{-11}	6.86×10^{-11}	4.67×10^{-11}	31.10%
	k_3	1.58×10^{-18}	6.28×10^{-19}	2.35×10^{-19}	8.26×10^{-20}	2.70×10^{-20}	0.00%
	k_4	4.55×10^{-15}	2.39×10^{-15}	1.21×10^{-15}	5.85×10^{-16}	2.69×10^{-16}	0.00%
	k_{totRAF}	3.62×10^{-10}	2.89×10^{-10}	2.10×10^{-10}	1.48×10^{-10}	1.02×10^{-10}	66.00%
TiO_2				Ph-R_{HAA}ben			
	k_1	1.09×10^{-11}	7.26×10^{-12}	4.71×10^{-12}	2.97×10^{-12}	1.81×10^{-12}	1.49%
	k_2	7.09×10^{-15}	3.71×10^{-15}	1.86×10^{-15}	8.94×10^{-16}	4.07×10^{-16}	0.00%
	k_3	2.12×10^{-15}	1.09×10^{-15}	5.39×10^{-16}	2.54×10^{-16}	1.13×10^{-16}	0.00%

	$k_{totHAAben}$	1.09×10^{-11}	7.26×10^{-12}	4.71×10^{-12}	2.97×10^{-12}	1.81×10^{-12}	1.49%
				Ph-R_{HAA}sub			
	k_7	1.88×10^{-10}	1.41×10^{-10}	1.03×10^{-10}	7.40×10^{-11}	5.21×10^{-11}	32.51%
	$k_{totHAAsub}$	1.88×10^{-10}	1.41×10^{-10}	1.03×10^{-10}	7.40×10^{-11}	5.21×10^{-11}	32.51%
	k_{tot}	5.61×10^{-10}	4.37×10^{-10}	3.17×10^{-10}	2.25×10^{-10}	1.56×10^{-10}	100.00%
				Ph-R_{RAF}			
	k_1	1.41×10^{-11}	9.64×10^{-12}	6.43×10^{-12}	4.18×10^{-12}	2.64×10^{-12}	0.27%
	k_2	2.69×10^{-9}	2.13×10^{-9}	1.66×10^{-9}	1.27×10^{-9}	9.62×10^{-10}	70.73%
	k_3	4.38×10^{-12}	2.82×10^{-12}	1.76×10^{-12}	1.07×10^{-12}	6.29×10^{-13}	0.08%
	k_4	5.01×10^{-11}	3.56×10^{-11}	2.48×10^{-11}	1.69×10^{-11}	1.12×10^{-11}	1.06%
	k_{totRAF}	2.76×10^{-9}	2.18×10^{-9}	1.69×10^{-9}	1.29×10^{-9}	9.76×10^{-10}	72.14%
Gas phase				Ph-R_{HAA}ben			
	k_1	2.56×10^{-11}	1.75×10^{-11}	1.17×10^{-11}	7.60×10^{-12}	4.81×10^{-12}	0.50%
	k_2	1.02×10^{-36}	9.93×10^{-38}	8.31×10^{-39}	5.85×10^{-40}	3.41×10^{-41}	0.00%
	k_3	9.16×10^{-13}	5.75×10^{-13}	3.50×10^{-13}	2.07×10^{-13}	1.18×10^{-13}	0.01%
	k_{totHAn}	2.65×10^{-11}	1.81×10^{-11}	1.21×10^{-11}	7.81×10^{-12}	4.93×10^{-12}	0.51%
				Ph-R_{HAA}sub			
	k_7	1.04×10^{-9}	8.24×10^{-10}	6.41×10^{-10}	4.91×10^{-10}	3.70×10^{-10}	27.34%
	$k_{totHAAsub}$	1.04×10^{-9}	8.24×10^{-10}	6.41×10^{-10}	4.91×10^{-10}	3.70×10^{-10}	27.34%
	k_{tot}	3.83×10^{-9}	3.02×10^{-9}	2.34×10^{-9}	1.79×10^{-9}	1.35×10^{-9}	100.00%
				Ph-R_{RAF}			
	k_1	2.45×10^{12}	2.49×10^{12}	2.52×10^{12}	2.55×10^{12}	2.59×10^{12}	5.65%
	k_2	6.19×10^{12}	6.19×10^{12}	6.19×10^{12}	6.18×10^{12}	6.17×10^{12}	13.86%
	k_3	6.71×10^{12}	6.77×10^{12}	6.83×10^{12}	6.90×10^{12}	6.96×10^{12}	15.32%
	k_4	5.20×10^{12}	5.15×10^{12}	5.09×10^{12}	5.04×10^{12}	4.98×10^{12}	11.41%
	k_{totRAF}	2.06×10^{13}	2.06×10^{13}	2.06×10^{13}	2.07×10^{13}	2.07×10^{13}	46.24%
Bulk water				Ph-R_{HAA}ben			
	k_1	7.14×10^{12}	7.50×10^{12}	7.90×10^{12}	8.32×10^{12}	8.78×10^{12}	17.70%
	k_2	2.51×10^{12}	3.00×10^{12}	3.57×10^{12}	4.27×10^{12}	5.10×10^{12}	8.01%

	k_3	5.21×10^{12}	5.43×10^{12}	5.66×10^{12}	5.91×10^{12}	6.19×10^{12}	12.69%
	$k_{totHAAben}$	1.49×10^{13}	1.59×10^{13}	1.71×10^{13}	1.85×10^{13}	2.01×10^{13}	38.40%
				Ph-R_{HAA}sub			
	k_7	6.42×10^{12}	6.63×10^{12}	6.85×10^{12}	7.09×10^{12}	7.35×10^{12}	15.36%
	$k_{totHAAsub}$	6.42×10^{12}	6.63×10^{12}	6.85×10^{12}	7.09×10^{12}	7.35×10^{12}	15.36%
	k_{tot}	4.18×10^{13}	4.32×10^{13}	4.46×10^{13}	4.63×10^{13}	4.81×10^{13}	100.00%
				4-HBA			
				4-HBA-R_{RAF}			
	k_1	1.95×10^{-15}	9.98×10^{-16}	4.90×10^{-16}	2.30×10^{-16}	1.02×10^{-16}	0.00%
	k_2	6.50×10^{-11}	4.65×10^{-11}	3.26×10^{-11}	2.23×10^{-11}	1.49×10^{-11}	34.34%
	k_3	5.74×10^{-15}	3.05×10^{-15}	1.55×10^{-15}	7.58×10^{-16}	3.52×10^{-16}	0.00%
	k_4	1.29×10^{-13}	7.55×10^{-14}	4.28×10^{-14}	2.33×10^{-14}	1.22×10^{-14}	0.05%
	k_5	1.34×10^{-14}	7.30×10^{-15}	3.83×10^{-15}	1.93×10^{-15}	9.26×10^{-16}	0.00%
	k_6	9.21×10^{-13}	5.75×10^{-13}	3.49×10^{-13}	2.05×10^{-13}	1.16×10^{-13}	0.37%
	k_{totRAF}	6.61×10^{-11}	4.72×10^{-11}	3.30×10^{-11}	2.25×10^{-11}	1.50×10^{-11}	34.76%
A-W				4-HBA-R_{HAA}ben			
	k_2	1.48×10^{-14}	8.12×10^{-15}	4.29×10^{-15}	2.18×10^{-15}	1.05×10^{-15}	0.00%
	k_3	1.99×10^{-12}	1.28×10^{-12}	7.99×10^{-13}	4.85×10^{-13}	2.84×10^{-13}	0.84%
	k_5	8.95×10^{-15}	4.83×10^{-15}	2.51×10^{-15}	1.25×10^{-15}	5.90×10^{-16}	0.00%
	k_6	1.11×10^{-14}	6.02×10^{-15}	3.15×10^{-15}	1.57×10^{-15}	7.50×10^{-16}	0.00%
	$k_{totHAAben}$	2.02×10^{-12}	1.30×10^{-12}	8.09×10^{-13}	4.90×10^{-13}	2.86×10^{-13}	0.84%
				4-HBA-R_{HAA}sub			
	k_7	5.57×10^{-16}	2.74×10^{-16}	1.29×10^{-16}	5.74×10^{-17}	2.42×10^{-17}	0.00%
	k_8	1.17×10^{-10}	8.53×10^{-11}	6.11×10^{-11}	4.28×10^{-11}	2.94×10^{-11}	64.39%
	$k_{totHAAsub}$	1.17×10^{-10}	8.53×10^{-11}	6.11×10^{-11}	4.28×10^{-11}	2.94×10^{-11}	64.39%
	k_{tot}	1.85×10^{-10}	1.34×10^{-10}	9.49×10^{-11}	6.59×10^{-11}	4.47×10^{-11}	100.00%
				4-HBA-R_{RAF}			
TiO_2	k_1	8.61×10^{-16}	4.29×10^{-16}	2.05×10^{-16}	9.31×10^{-17}	4.01×10^{-17}	0.00%
	k_2	2.38×10^{-13}	1.42×10^{-13}	8.21×10^{-14}	4.59×10^{-14}	2.46×10^{-14}	0.00%

	k_3	5.00×10^{-15}	2.64×10^{-15}	1.34×10^{-15}	6.51×10^{-16}	3.01×10^{-16}	0.00%
	k_4	4.72×10^{-9}	3.88×10^{-9}	3.16×10^{-9}	2.54×10^{-9}	2.01×10^{-9}	99.96%
	k_5	5.36×10^{-16}	2.63×10^{-16}	1.24×10^{-16}	5.52×10^{-17}	2.33×10^{-17}	0.00%
	k_6	3.71×10^{-14}	2.09×10^{-14}	1.14×10^{-14}	5.96×10^{-15}	2.98×10^{-15}	0.00%
	k_{totRAF}	4.72×10^{-9}	3.88×10^{-9}	3.16×10^{-9}	2.54×10^{-9}	2.01×10^{-9}	99.96%
	4-HBA-R_{HAA}ben						
	k_2	1.62×10^{-14}	8.90×10^{-15}	4.71×10^{-15}	2.39×10^{-15}	1.15×10^{-15}	0.00%
	k_3	1.52×10^{-15}	7.76×10^{-16}	3.78×10^{-16}	1.76×10^{-16}	7.72×10^{-17}	0.00%
	k_5	1.98×10^{-13}	1.19×10^{-13}	6.86×10^{-14}	3.83×10^{-14}	2.05×10^{-14}	0.00%
	k_6	9.78×10^{-17}	4.55×10^{-17}	2.01×10^{-17}	8.42×10^{-18}	3.32×10^{-18}	0.00%
	$k_{totHAAben}$	2.16×10^{-13}	1.29×10^{-13}	7.37×10^{-14}	4.09×10^{-14}	2.17×10^{-14}	0.00%
	4-HBA-R_{HAA}sub						
	k_7	1.34×10^{-12}	8.44×10^{-13}	5.16×10^{-13}	3.05×10^{-13}	1.74×10^{-13}	0.02%
	k_8	1.22×10^{-12}	7.71×10^{-13}	4.75×10^{-13}	2.83×10^{-13}	1.63×10^{-13}	0.02%
	$k_{totHAAsub}$	2.56×10^{-12}	1.62×10^{-12}	9.91×10^{-13}	5.88×10^{-13}	3.37×10^{-13}	0.04%
	k_{tot}	4.72×10^{-9}	3.88×10^{-9}	3.16×10^{-9}	2.54×10^{-9}	2.01×10^{-9}	100.00%
	4-HBA-R_{RAF}						
	k_1	1.99×10^{-14}	1.10×10^{-14}	5.84×10^{-15}	2.98×10^{-15}	1.45×10^{-15}	0.01%
	k_2	2.57×10^{-12}	1.66×10^{-12}	1.04×10^{-12}	6.34×10^{-13}	3.74×10^{-13}	1.32%
	k_3	1.25×10^{-14}	6.81×10^{-15}	3.57×10^{-15}	1.79×10^{-15}	8.57×10^{-16}	0.00%
	k_4	2.21×10^{-14}	1.22×10^{-14}	6.53×10^{-15}	3.34×10^{-15}	1.63×10^{-15}	0.01%
	k_5	2.90×10^{-15}	1.50×10^{-15}	7.49×10^{-16}	3.56×10^{-16}	1.61×10^{-16}	0.00%
Gas-phase	k_6	4.64×10^{-14}	2.63×10^{-14}	1.44×10^{-14}	7.59×10^{-15}	3.82×10^{-15}	0.02%
	k_{totRAF}	2.67×10^{-12}	1.72×10^{-12}	1.07×10^{-12}	6.50×10^{-13}	3.82×10^{-13}	1.36%
	4-HBA-R_{HAA}ben						
	k_2	5.70×10^{-14}	3.27×10^{-14}	1.81×10^{-14}	9.63×10^{-15}	4.91×10^{-15}	0.02%
	k_3	6.73×10^{-15}	3.60×10^{-15}	1.85×10^{-15}	9.09×10^{-16}	4.25×10^{-16}	0.00%
	k_5	7.77×10^{-14}	4.49×10^{-14}	2.50×10^{-14}	1.34×10^{-14}	6.90×10^{-15}	0.03%
	k_6	4.93×10^{-40}	3.89×10^{-41}	2.59×10^{-42}	1.43×10^{-43}	6.41×10^{-45}	0.00%

	$k_{totHAAben}$	1.41×10^{-13}	8.12×10^{-14}	4.50×10^{-14}	2.39×10^{-14}	1.22×10^{-14}	0.05%
				4-HBA-R_{HAA}sub			
	k_7	5.84×10^{-12}	3.88×10^{-12}	2.51×10^{-12}	1.58×10^{-12}	9.61×10^{-13}	3.18%
	k_8	1.42×10^{-10}	1.04×10^{-10}	7.53×10^{-11}	5.32×10^{-11}	3.68×10^{-11}	95.41%
	$k_{totHAAsub}$	1.48×10^{-10}	1.08×10^{-10}	7.78×10^{-11}	5.48×10^{-11}	3.78×10^{-11}	98.59%
	k_{tot}	1.51×10^{-10}	1.10×10^{-10}	$7.90\times10_{-11}$	5.55×10^{-11}	3.81×10^{-11}	100.00%
				4-HBA-R_{RAF}			
	k_1	1.34×10^{12}	1.39×10^{12}	1.44×10^{12}	1.49×10^{12}	1.55×10^{12}	5.71%
	k_2	1.62×10^{12}	1.66×10^{12}	1.69×10^{12}	1.73×10^{12}	1.76×10^{12}	6.71%
	k_3	1.72×10^{12}	1.77×10^{12}	1.83×10^{12}	1.88×10^{12}	1.94×10^{12}	7.25%
	k_4	2.13×10^{12}	2.17×10^{12}	2.20×10^{12}	2.24×10^{12}	2.28×10^{12}	8.75%
	k_5	2.09×10^{12}	2.14×10^{12}	2.20×10^{12}	2.26×10^{12}	2.32×10^{12}	8.73%
	k_6	2.60×10^{12}	2.64×10^{12}	2.68×10^{12}	2.71×10^{12}	2.75×10^{12}	10.62%
	k_{totRAF}	1.15×10^{13}	1.18×10^{13}	1.20×10^{13}	1.23×10^{13}	1.26×10^{13}	47.77%
Bulk water				4-HBA-R_{HAA}ben			
	k_2	2.14×10^{12}	2.30×10^{12}	2.47×10^{12}	2.65×10^{12}	2.86×10^{12}	9.80%
	k_3	4.13×10^{10}	5.02×10^{10}	6.12×10^{10}	7.48×10^{10}	9.14×10^{10}	0.24%
	k_5	4.24×10^{12}	4.52×10^{12}	4.82×10^{12}	5.15×10^{12}	5.50×10^{12}	19.13%
	k_6	3.54×10^{11}	4.33×10^{11}	5.30×10^{11}	6.50×10^{11}	7.98×10^{11}	2.10%
	$k_{totHAAben}$	6.78×10^{12}	7.30×10^{12}	7.88×10^{12}	8.52×10^{12}	9.25×10^{12}	31.27%
				4-HBA-R_{HAA}sub			
	k_7	1.90×10^{12}	2.08×10^{12}	2.28×10^{12}	2.51×10^{12}	2.76×10^{12}	9.06%
	k_8	2.99×10^{12}	3.00×10^{12}	3.00×10^{12}	3.00×10^{12}	3.00×10^{12}	11.90%
	$k_{totHAAsub}$	4.89×10^{12}	5.08×10^{12}	5.28×10^{12}	5.51×10^{12}	5.76×10^{12}	20.96%
	k_{tot}	2.32×10^{13}	2.41×10^{13}	2.52×10^{13}	2.63×10^{13}	2.76×10^{13}	100.00%
				VL			
				VL-R_{RAF}			
A-W	k_1	7.87×10^{-11}	5.67×10^{-11}	4.00×10^{-11}	2.77×10^{-11}	1.87×10^{-11}	0.02%
	k_2	1.15×10^{-11}	7.78×10^{-12}	5.15×10^{-12}	3.32×10^{-12}	2.08×10^{-12}	0.00%

	k_3	1.96×10^{-9}	1.57×10^{-9}	1.24×10^{-9}	9.69×10^{-10}	7.44×10^{-10}	0.72%
	k_4	2.10×10^{-8}	1.81×10^{-8}	1.55×10^{-8}	1.31×10^{-8}	1.10×10^{-8}	8.98%
	k_5	5.13×10^{-8}	4.55×10^{-8}	4.02×10^{-8}	3.52×10^{-8}	3.06×10^{-8}	23.27%
	k_6	1.28×10^{-9}	1.01×10^{-9}	7.88×10^{-10}	6.04×10^{-10}	4.55×10^{-10}	0.46%
	k_{totRAF}	7.57×10^{-8}	6.63×10^{-8}	5.77×10^{-8}	4.99×10^{-8}	4.29×10^{-8}	33.46%
				VL-R_{HAA}ben			
	k_3	7.17×10^{-14}	4.13×10^{-14}	2.30×10^{-14}	1.23×10^{-14}	6.30×10^{-15}	0.00%
	k_5	5.47×10^{-13}	3.37×10^{-13}	2.02×10^{-13}	1.17×10^{-13}	6.49×10^{-14}	0.00%
	k_6	2.33×10^{-13}	1.38×10^{-13}	7.98×10^{-14}	4.43×10^{-14}	2.37×10^{-14}	0.00%
	$k_{totHAAben}$	8.51×10^{-13}	5.17×10^{-13}	3.04×10^{-13}	1.73×10^{-13}	9.49×10^{-14}	0.00%
				VL-R_{HAA}sub			
	k_7	2.99×10^{-10}	2.23×10^{-10}	1.64×10^{-10}	1.18×10^{-10}	8.31×10^{-11}	0.10%
	k_8	1.35×10^{-7}	1.25×10^{-7}	1.14×10^{-7}	1.05×10^{-7}	9.51×10^{-8}	66.36%
	k_9	2.78×10^{-10}	2.10×10^{-10}	1.56×10^{-10}	1.14×10^{-10}	8.11×10^{-11}	0.09%
	$k_{totHAAsub}$	1.36×10^{-7}	1.25×10^{-7}	1.15×10^{-7}	1.05×10^{-7}	9.53×10^{-8}	66.54%
	k_{tot}	2.12×10^{-7}	1.91×10^{-7}	1.73×10^{-7}	1.55×10^{-7}	1.38×10^{-7}	100.00%
				VL-R_{RAF}			
	k_1	3.78×10^{-7}	3.59×10^{-7}	3.42×10^{-7}	3.25×10^{-7}	3.09×10^{-7}	5.11%
	k_2	3.39×10^{-7}	3.21×10^{-7}	3.04×10^{-7}	2.87×10^{-7}	2.71×10^{-7}	4.53%
	k_3	3.47×10^{-7}	3.29×10^{-7}	3.12×10^{-7}	2.95×10^{-7}	2.78×10^{-7}	4.65%
	k_4	3.18×10^{-7}	3.00×10^{-7}	2.82×10^{-7}	2.66×10^{-7}	2.49×10^{-7}	4.22%
TiO_2	k_5	3.77×10^{-7}	3.59×10^{-7}	3.42×10^{-7}	3.25×10^{-7}	3.09×10^{-7}	5.11%
	k_6	3.58×10^{-7}	3.40×10^{-7}	3.23×10^{-7}	3.06×10^{-7}	2.90×10^{-7}	4.82%
	k_{totRAF}	2.12×10^{-6}	2.01×10^{-6}	1.91×10^{-6}	1.80×10^{-6}	1.71×10^{-6}	28.44%
				VL-R_{HAA}ben			
	k_3	1.28×10^{-18}	5.16×10^{-19}	1.96×10^{-19}	7.00×10^{-20}	2.32×10^{-20}	0.00%
	k_5	9.66×10^{-7}	9.47×10^{-7}	9.30×10^{-7}	9.13×10^{-7}	8.97×10^{-7}	13.88%
	k_6	9.35×10^{-7}	9.17×10^{-7}	9.00×10^{-7}	8.83×10^{-7}	8.67×10^{-7}	13.44%
	$k_{totHAAben}$	1.90×10^{-6}	1.86×10^{-6}	1.83×10^{-6}	1.80×10^{-6}	1.76×10^{-6}	27.32%

				VL-R_{HAA}sub			
	k_7	2.55×10^{-6}	2.53×10^{-6}	2.52×10^{-6}	2.50×10^{-6}	2.49×10^{-6}	37.59%
	k_8	4.00×10^{-15}	2.09×10^{-15}	1.05×10^{-15}	5.02×10^{-16}	2.28×10^{-16}	0.00%
	k_9	4.81×10^{-7}	4.63×10^{-7}	4.46×10^{-7}	4.29×10^{-7}	4.13×10^{-7}	6.65%
	$k_{totHAAsub}$	3.03×10^{-6}	2.99×10^{-6}	2.97×10^{-6}	2.93×10^{-6}	2.90×10^{-6}	44.24%
	k_{tot}	7.05×10^{-6}	6.87×10^{-6}	6.70×10^{-6}	6.53×10^{-6}	6.37×10^{-6}	100.00%
				VL-R_{RAF}			
	k_1	1.27×10^{-12}	7.97×10^{-13}	4.88×10^{-13}	2.89×10^{-13}	1.66×10^{-13}	0.43%
	k_2	1.34×10^{-11}	9.12×10^{-12}	6.06×10^{-12}	3.93×10^{-12}	2.47×10^{-12}	5.30%
	k_3	1.75×10^{-12}	1.11×10^{-12}	6.91×10^{-13}	4.16×10^{-13}	2.42×10^{-13}	0.60%
	k_4	1.16×10^{-13}	6.77×10^{-14}	3.81×10^{-14}	2.06×10^{-14}	1.07×10^{-14}	0.03%
	k_5	2.00×10^{-14}	1.10×10^{-14}	5.82×10^{-15}	2.95×10^{-15}	1.43×10^{-15}	0.01%
	k_6	2.71×10^{-14}	1.51×10^{-14}	8.08×10^{-15}	4.16×10^{-15}	2.04×10^{-15}	0.01%
	k_{totRAF}	1.66×10^{-11}	1.11×10^{-11}	7.29×10^{-12}	4.66×10^{-12}	2.89×10^{-12}	6.38%
				VL-R_{HAA}ben			
Gas phase	k_3	1.76×10^{-29}	3.07×10^{-30}	4.77×10^{-31}	6.50×10^{-32}	7.69×10^{-33}	0.00%
	k_5	6.93×10^{-14}	3.99×10^{-14}	2.22×10^{-14}	1.18×10^{-14}	6.05×10^{-15}	0.02%
	k_6	2.37×10^{-38}	2.11×10^{-39}	1.60×10^{-40}	1.02×10^{-41}	5.30×10^{-43}	0.00%
	$k_{totHAAben}$	6.93×10^{-14}	3.99×10^{-14}	2.22×10^{-14}	1.18×10^{-14}	6.05×10^{-15}	0.02%
				VL-R_{HAA}sub			
	k_7	9.26×10^{-13}	5.79×10^{-13}	3.51×10^{-13}	2.06×10^{-13}	1.17×10^{-13}	0.31%
	k_8	1.95×10^{-10}	1.46×10^{-10}	1.07×10^{-10}	7.69×10^{-11}	5.42×10^{-11}	93.30%
	k_9	1.98×10^{-14}	1.09×10^{-14}	5.78×10^{-15}	2.94×10^{-15}	1.43×10^{-15}	0.01%
	$k_{totHAAsub}$	1.96×10^{-10}	1.47×10^{-10}	1.07×10^{-10}	7.71×10^{-11}	5.43×10^{-11}	93.62%
	k_{tot}	2.12×10^{-10}	1.57×10^{-10}	1.14×10^{-10}	8.18×10^{-11}	5.73×10^{-11}	100.00%
				VL-R_{RAF}			
	k_1	2.45×10^{12}	2.47×10^{12}	2.49×10^{12}	2.50×10^{12}	2.51×10^{12}	7.90%
	k_2	2.60×10^{12}	2.63×10^{12}	2.65×10^{12}	2.67×10^{12}	2.69×10^{12}	8.41%
Bulk water	k_3	2.24×10^{12}	2.28×10^{12}	2.31×10^{12}	2.35×10^{12}	2.38×10^{12}	7.34%

k_4	1.98×10^{12}	1.99×10^{12}	2.01×10^{12}	2.02×10^{12}	2.02×10^{12}	6.37%
k_5	2.20×10^{12}	2.21×10^{12}	2.22×10^{12}	2.22×10^{12}	2.22×10^{12}	7.05%
k_6	2.11×10^{12}	2.14×10^{12}	2.16×10^{12}	2.19×10^{12}	2.21×10^{12}	6.88%
k_{totRAF}	1.36×10^{13}	1.37×10^{13}	1.38×10^{13}	1.40×10^{13}	1.40×10^{13}	43.95%
			VL-R_{HAA}ben			
k_3	1.08×10^{12}	1.27×10^{12}	1.49×10^{12}	1.75×10^{12}	2.07×10^{12}	4.73%
k_5	3.83×10^{12}	4.09×10^{12}	4.38×10^{12}	4.69×10^{12}	5.02×10^{12}	13.90%
k_6	8.04×10^{11}	9.63×10^{11}	1.15×10^{12}	1.38×10^{12}	1.66×10^{12}	3.66%
$k_{totHAAben}$	5.71×10^{12}	6.32×10^{12}	7.02×10^{12}	7.82×10^{12}	8.75×10^{12}	22.29%
			VL-R_{HAA}sub			
k_7	4.52×10^{12}	4.84×10^{12}	5.18×10^{12}	5.55×10^{12}	5.96×10^{12}	16.45%
k_8	3.75×10^{12}	3.84×10^{12}	3.93×10^{12}	4.03×10^{12}	4.14×10^{12}	12.49%
k_9	1.45×10^{12}	1.48×10^{12}	1.51×10^{12}	1.55×10^{12}	1.58×10^{12}	4.81%
$k_{totHAAsub}$	9.72×10^{12}	1.02×10^{13}	1.06×10^{13}	1.11×10^{13}	1.17×10^{13}	33.75%
k_{tot}	2.90×10^{13}	3.02×10^{13}	3.15×10^{13}	3.29×10^{13}	3.45×10^{13}	100.00%

Table S7. The acute and chronic toxicity of Ph, 4-HBA, VL and their products. (mg L^{-1})

Classification	Acute toxicity[1]	Chronic toxicity[2]
Not harmful	LC_{50}>100 or EC_{50}>100	ChV>10
Harmful	10< LC_{50} <100 or 10< EC_{50} <100	1< ChV <10
Toxic	1< LC_{50} <10 or 1< EC_{50} <10	0.1< ChV <1
Very toxic	LC_{50} <1 or EC_{50} <1	ChV<0.1

[1] Criteria set by the European Union (described in Annex VI of Directive 67/548/EEC); [2]Criteria set by the Chinese hazard evaluation guidelines for new chemical substances (HJ/T 154–2004).

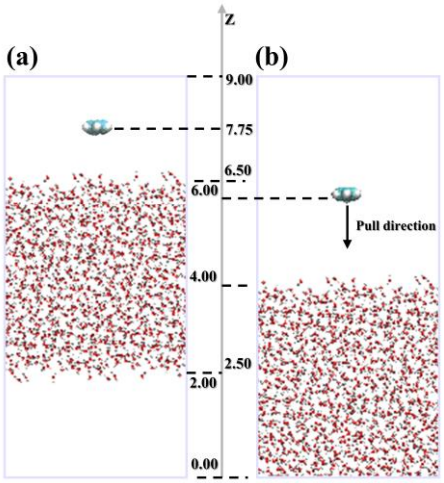

Fig. S1 Schematic representation the initial configuration of **(a)** the umbrella sampling simulation and **(b)** the 150 ns NVT simulation (unit: nm).

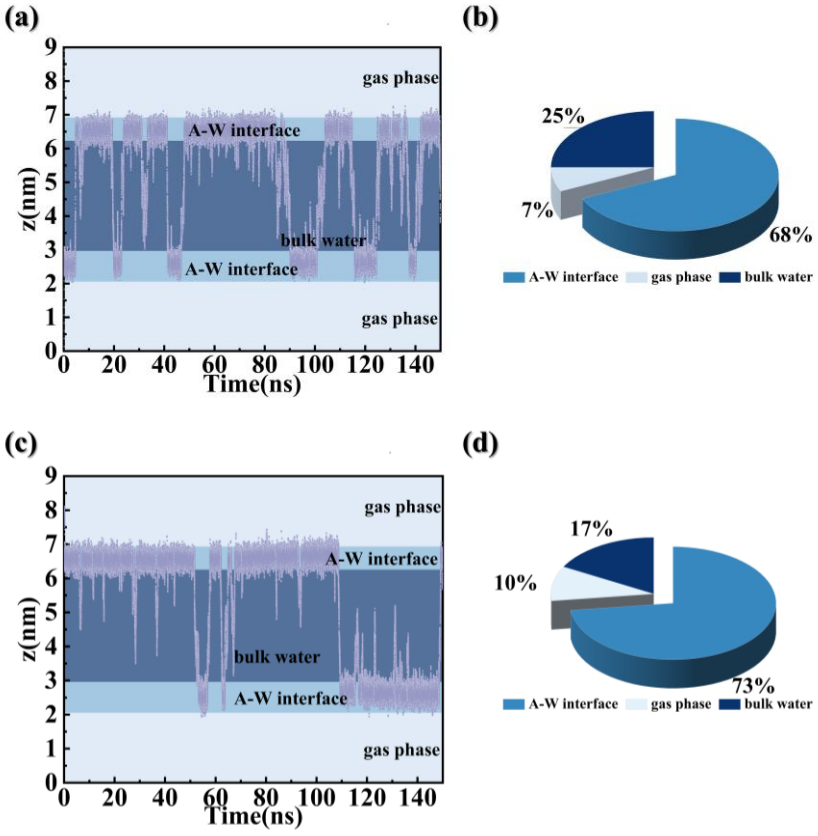

Fig S2 The z coordinates of **(a)** 4-HBA and **(c)** as the function of 150 ns simulation time; the pie chart with the probability of **(b)** O_3 and **(d)** Ph at the A-W interface, in air, and in bulk water.

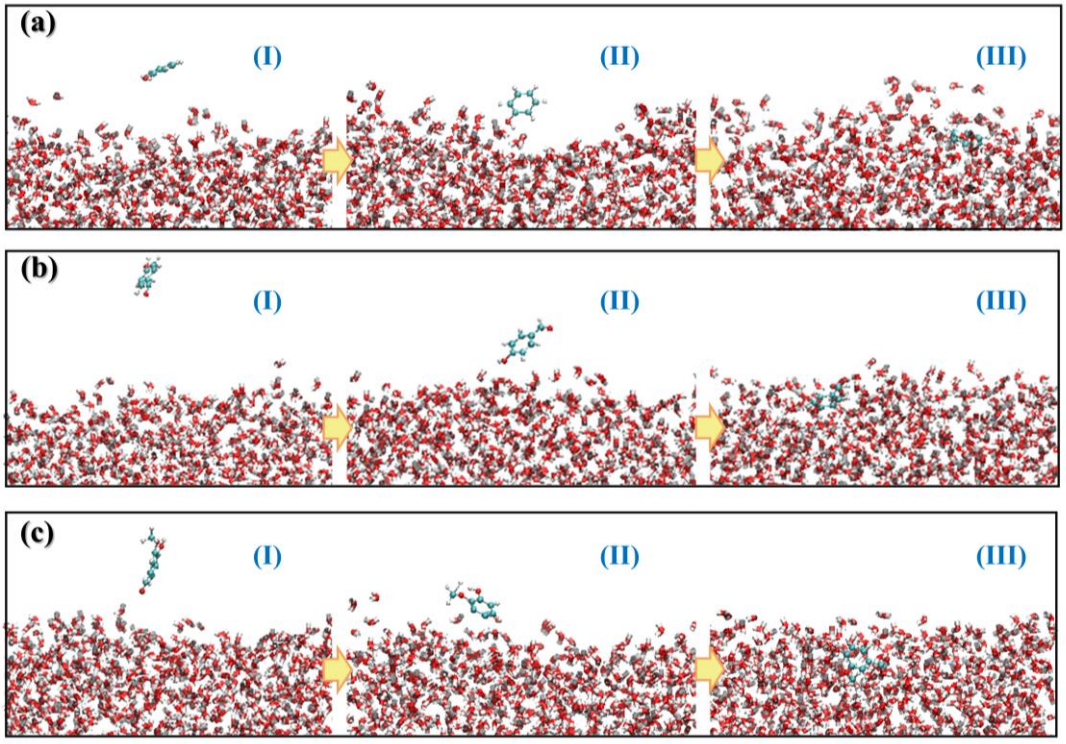

Fig. S3 Typical snapshots from the trajectories of **(a)** Ph, **(b)** 4-HBA, and **(c)** VL diffuse through the interior of the water slab from the air region.

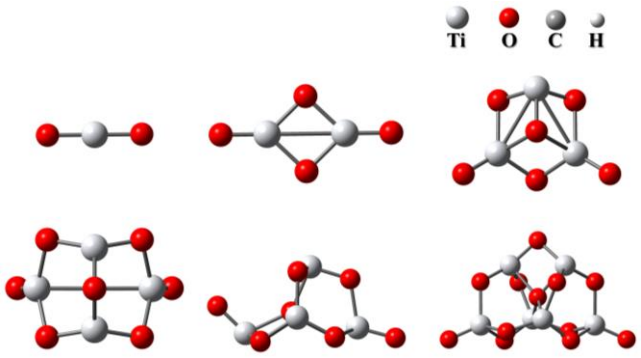

Fig. S4 The minimum energy structures of $(TiO_2)_n$ (n = 1–6) obtained at the M06-2X/ 6-31 + g(d,p)/LANL2DZ level.

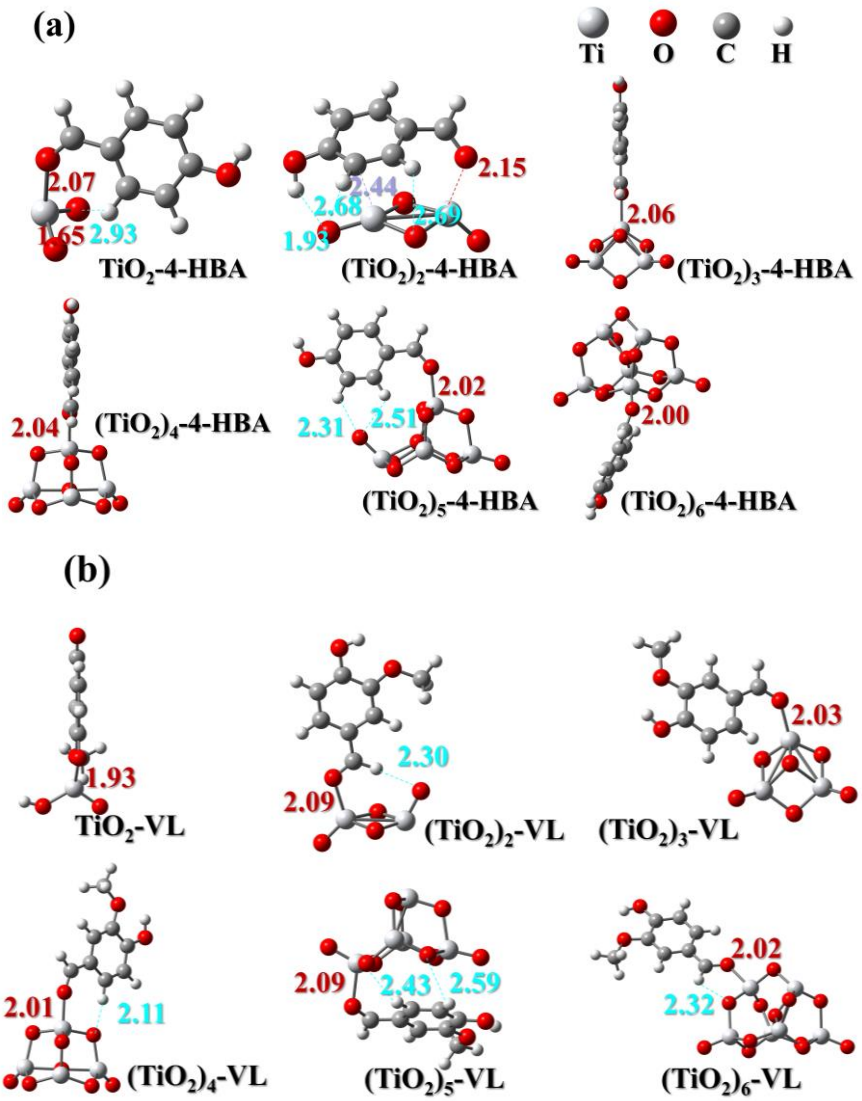

Fig. S5 The minimum energy structures of six $(TiO_2)_n$ (n = 1–6) obtained at the M06-2X / 6-31 + g(d,p) / LANL2DZ level.

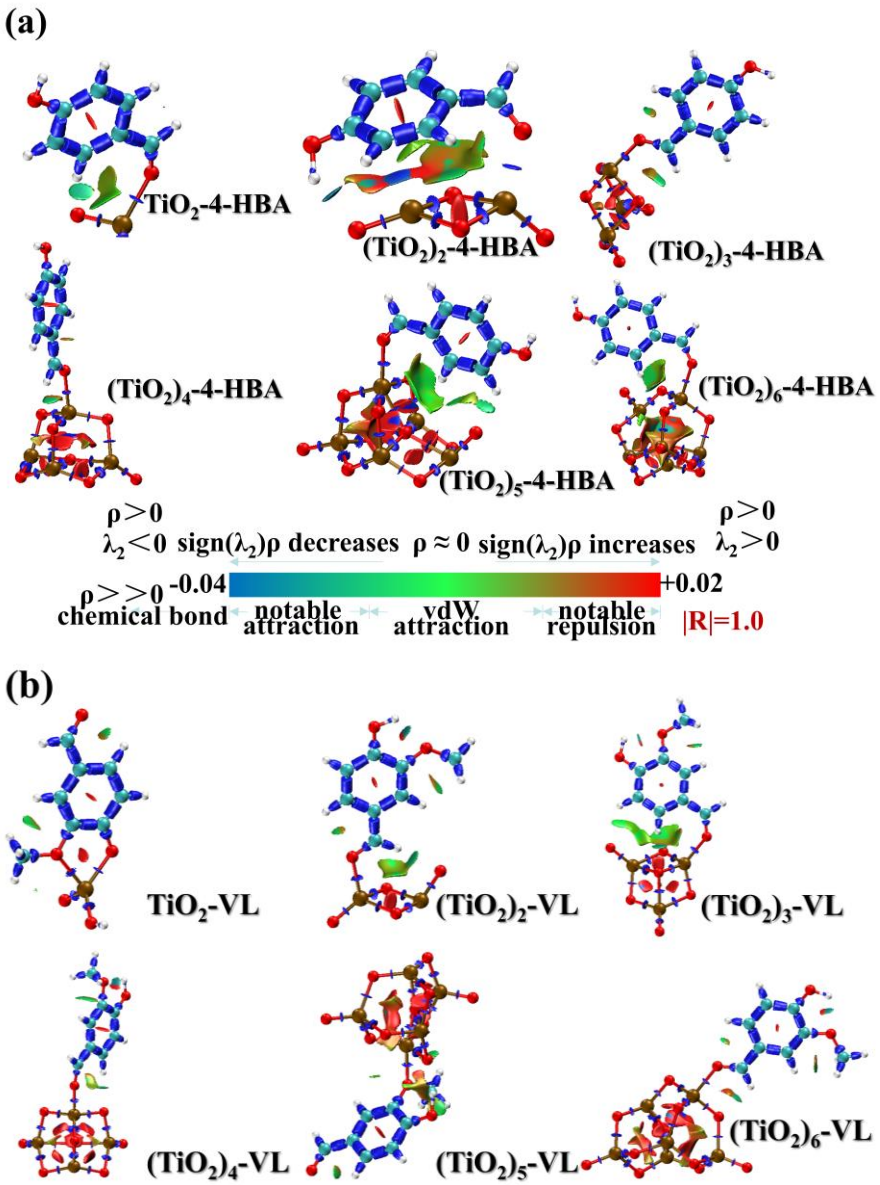

Fig. S6 Interaction region indicator (IRI) analyses of **(a)** 4-HBA and **(b)** VL on $(TiO_2)_n$ (n = 1 – 6) surface.

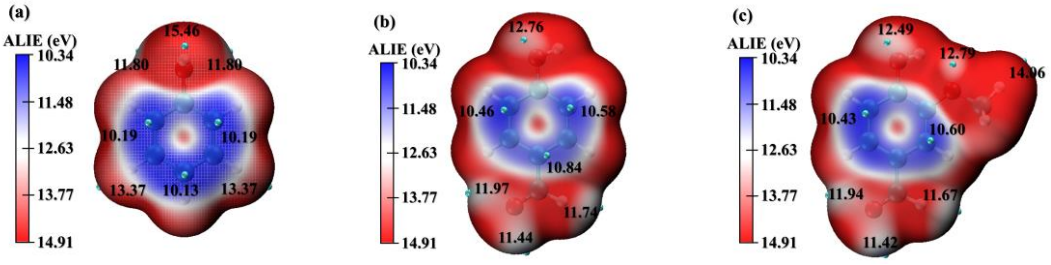

Fig. S7 The average local ionization energy (ALIE) of Ph, 4-HBA, and VL.

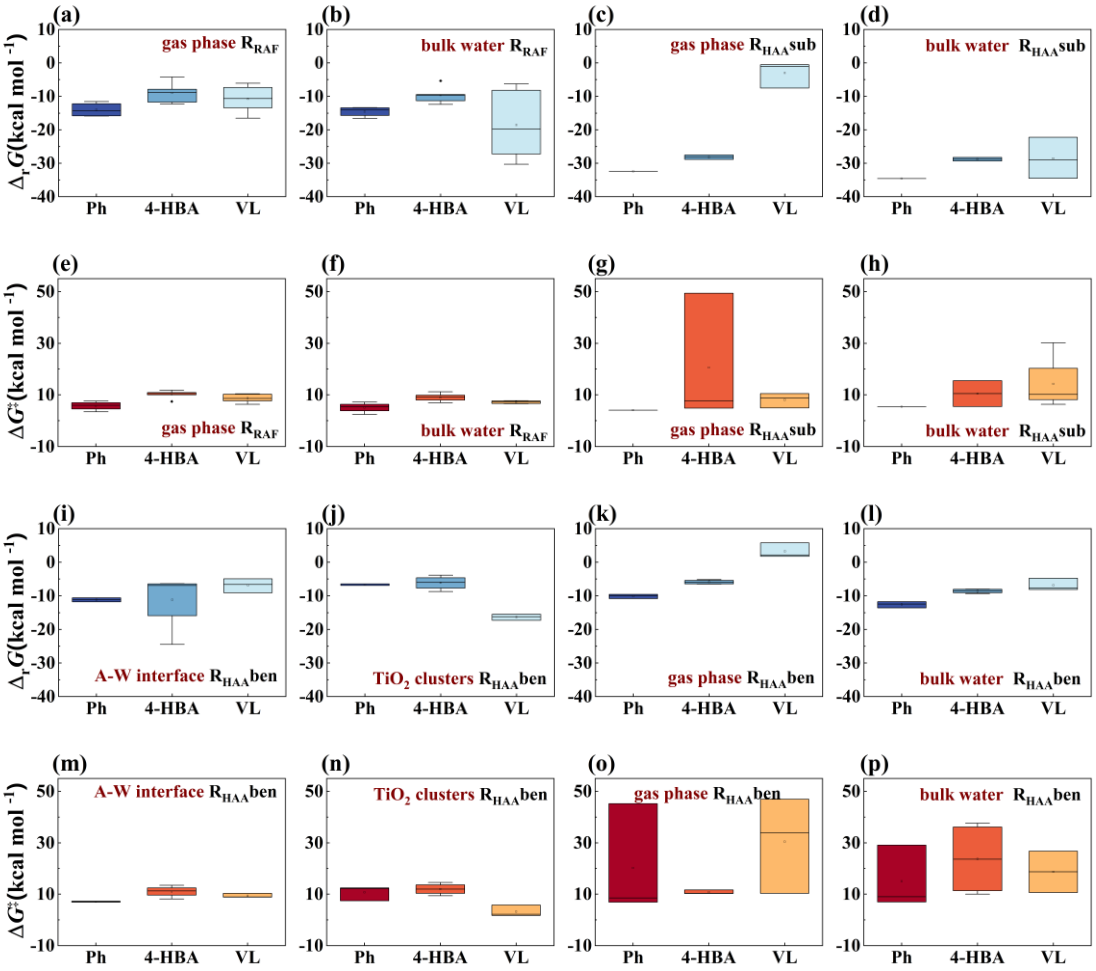

Fig. S8 Statistical charts of calculated **(a)** – **(d)** $\Delta_r G$ and **(e)** – **(h)** $\Delta G^{\ddagger}$ values for O_3-initiated reactions; **(i)** – **(l)** $\Delta_r G$ and **(m)** – **(p)** $\Delta G^{\ddagger}$ values for $HO^{\bullet}$ -initiated reactions.

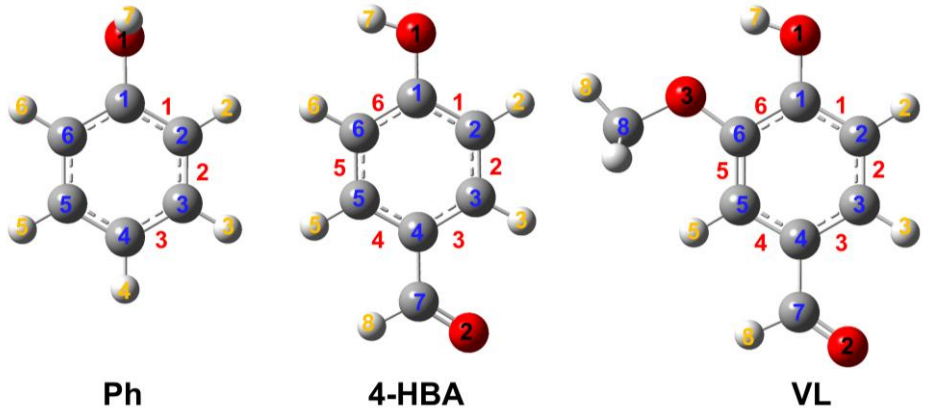

Fig. S9 Minimum free energy structures of the Ph/4-HBA/VL at the SMD/M06-2X/6-31+*G*(d,p) level of theory.

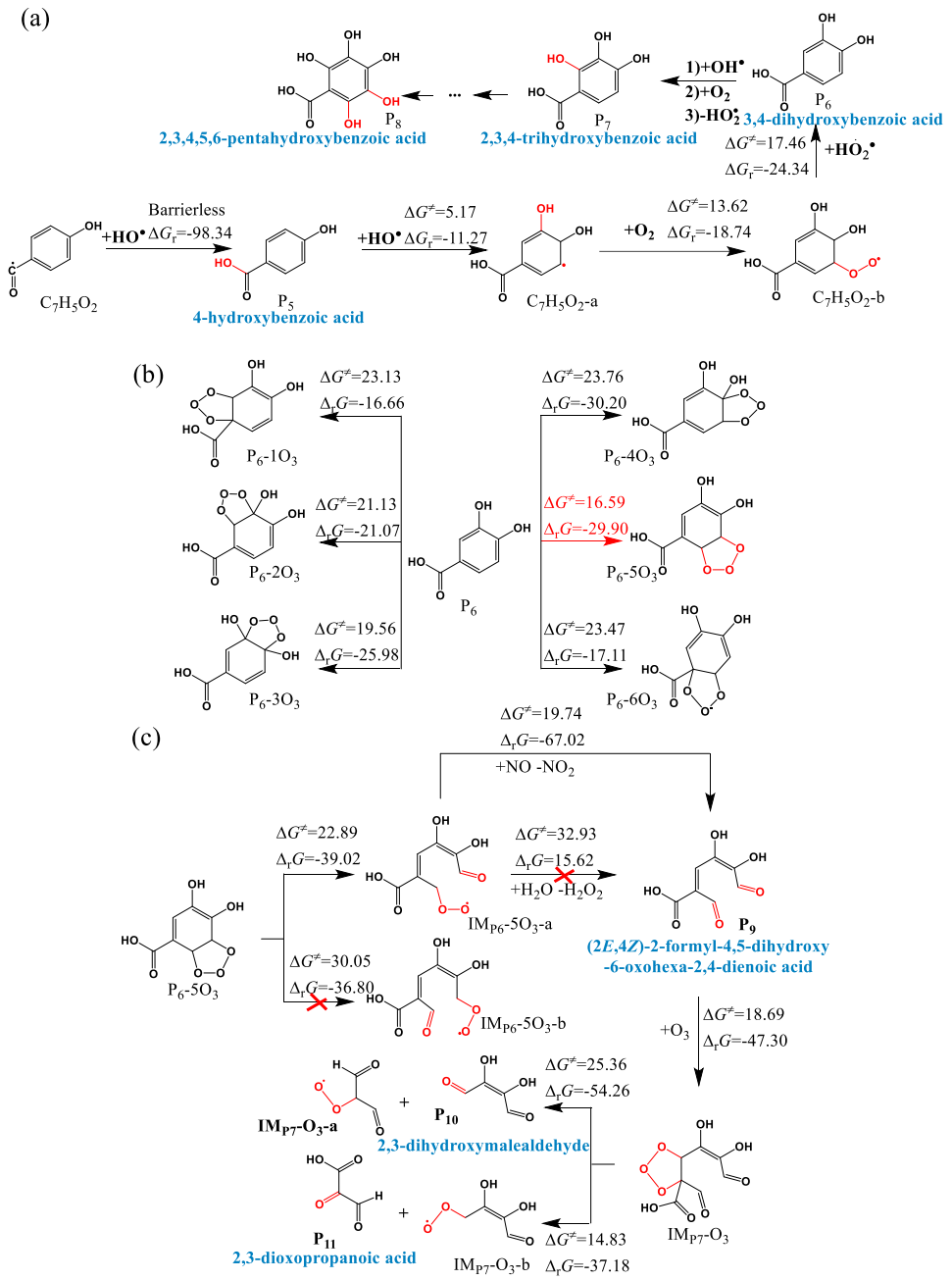

Fig. S10 The subsequent reaction mechanisms of important intermediates (IMs) at A-W interface. Unit in kcal mol $^{-1}$.

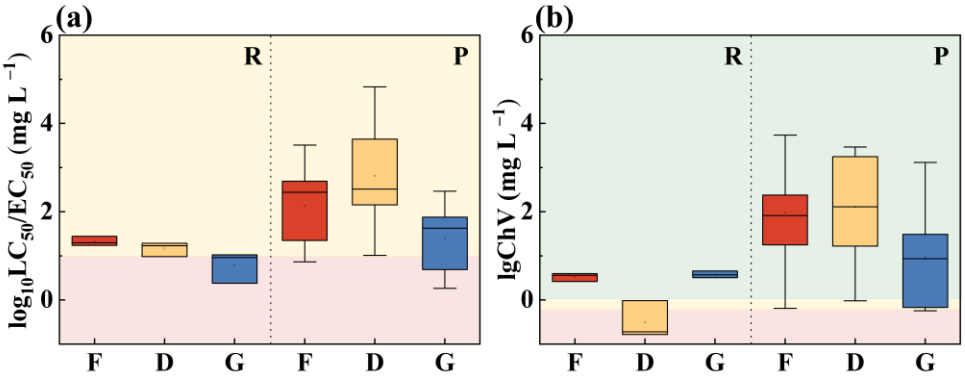

Fig. S11 (a) aquatic acute toxicity and **(b)** chronic toxicity of Ph, 4-HBA, and VL and their oxidation products. F: fish; D: daphnid; G: green algae.

Text S1. The simulation details of umbrella sampling simulations.

For each system, a short relax simulation (2 ns) with the position restraint of the Ph (or 4-HBA or VL) was performed using the NVT ensemble after the completion of the energy minimization. The water molecule with the COM coordinate (2.0 nm, 2.0 nm, 1.5 nm) was chosen as the pull reference group. To obtain the umbrella windows, a 400 ps pull simulation was performed. The Ph (or 4-HBA or VL) molecule was pull towards the COM of the water slab along with z direction at a rate of 0.005 nm ps^{-1} and the pull force constant of 1000 kJ mol^{-1} nm^{-2}. The position of Ph (or 4-HBA, or VL) was restrained in order to on the one hand eliminate the effect of its movement in x and y directions on the reaction coordinate, and on the other hand allow the rotational of the molecule in the pull process. There were 70 windows in the umbrella sampling (US) simulations (Kästner, 2011) and the bound of the R in every window was kept the same as $Z \in [0, 4.0\ nm]$. The distance was varied by steps of 0.05 nm, centered from 4.0 nm to 0 nm.

Text S2. The radial distribution function and coordination number

The radial distribution function (RDF) can be used to estimate the hydrogen bonding (HB) strength between particular atoms. The HB between Ph (4-HBA, or VL) and water at air-water interfaces occurs. The number of water molecules around the Ph (4-HBA, or VL) molecule was obtained by calculating the coordination number (N). Considering the density at the interface is equal to 50% of the nanoparticle interior, the N parameter is obtained as the integrations of g(r) within r=2.5 Å.

Text S3. Details of DFT calculations

The geometry optimizations and harmonic vibrational frequency of all species were determined at the M06–2X/6-31 + G(d,p) level for the gas phase. Intrinsic reaction coordinate calculations (IRCs) were used to confirm each transition state (TS) connecting the reactants (Rs) and products (Ps). The single-point energy calculations were performed at a higher level — M06–2X/6–311++G(3df,2p). The continuum solvation model 'SMD' was used to consider the solvent effect of the bulk water. The reliability of the theoretical level we have chosen has been proved in previous studies (Wang et al., 2021b). The M06-2X/6-31+G(d, p) level for C, O, and H (Yan and Truhlar, 2015; Zhao and Truhlar, 2008a, b) and M06-2X/LANL2DZ level (Hay and Wadt, 1985a; Wadt and Hay, 1985; Hay and Wadt, 1985b) for Ti were used to obtain credible results (An et al., 2021). Fu et al. (Fu et al., 2020) and Wang et al. (Wang et al., 2021a) have used various levels of theory to verify the accuracy of this level. According to previous studies, the LanL2DZ basis set performs well in calculating transition metals (Qu et al., 2018). The geometry optimizations and vibrational frequencies for all reactants (Rs), transition states (TSs), intermediates (IMs), and products (Ps) were obtained. Intrinsic reaction coordinate (IRC) was also used to confirm the correctness of the TSs. Besides, M06-2X/6-311++G(3df,2p)/LANL2TZ (Hay and Wadt, 1985a; Roy et al., 2008) was used to receive single-point energy. At 298 K and 1 atm, Gibbs free energy was obtained. Besides, the free energy corrections also were considered. The adsorption Gibbs free energy was calculated by Eq. (1):

$\Delta G_{ad} = G_{adsorption\ complex} - G_{isolated\ molecule} - G_{surface\ model}$ (1)

Where $\Delta G_{adsorption\ complex}$ is the total energy of the adsorbate-surface complex; $G_{isolated\ molecule}$ is the energy of Ph (or 4-HBA or VL); $G_{surface\ model}$ is the energy of $(TiO_2)_n$ (n = 1-6) clusters.

Text S4. Interaction region indicator (IRI).

$$\mathrm{IRI(r)} = \frac{|\nabla\rho(r)|}{[\rho(r)]^{1.0}} \quad (2)$$

where a is an adjustable parameter, a=1.1 is adopted for standard definition of IRI. IRI is essentially the gradient norm of electron density weighted by scaled electron density. Note that if a=4/3, IRI only differs from RDG by a constant prefactor. Obviously, IRI can be immediately implemented in any code that already supported RDG. As will be shown, by properly choosing isovalue, isosurfaces of IRI are able to exhibit various kinds of interaction regions.

Visual Molecular Dynamics (version 1.9.3) (Humphrey et al., 1996) was used to display the results.

Text S5. Calculation of reaction rate constant.

Chemical reaction process should be considered in the calculation of bimolecular reaction rate constant (k_i) of each elementary reaction (i). The chemical reaction rate constant (k_{chem}) of each reaction route was calculated using conventional transition state theory:

$$k_{chem} = \sigma\kappa\frac{k_B T}{h}K^0 e^{\frac{-\Delta G^{\neq}}{RT}} \quad (3)$$

where k_B and h were the Boltzmann and Planck constants respectively; T was the temperature; R was the gas constant; $\Delta G^{\ddagger}$ was the free energy barrier including the thermodynamic contribution correction; σ was the reaction path degeneracy, accounting for the number of equivalent reaction paths.

Text S6. Interfacial adsorption properties

To identify the ability of the interface to adsorb gaseous phenolic compounds (Ph, 4-HBA, or VL), the free energy difference from gaseous phenolic compounds (Ph, 4-HBA, or VL) to the interface is defined as: $\Delta G_{gas \rightarrow interface} = G_{interface} - G_{gas}$, where $G_{interface}$ refers to the minimum value at the interface and G_{gas} is the maximum value in the gas phase. The corresponding value reflects whether the interface prefers to adsorb gaseous phenolic compounds (Ph, 4-HBA, or VL).

References

An, Z., Li, M., Huo, Y., Jiang, J., Zhou, Y., Jin, Z., Xie, J., Zhan, J., and He, M.: The pH-dependent contributions of radical species during the removal of aromatic acids and bases in light/chlorine systems, Chem. Eng. J., 133493, https://doi.org/10.1016/j.cej.2021.133493, 2021.

Fu, Z., Xie, H.-B., Elm, J., Guo, X., Fu, Z., and Chen, J.: Formation of Low-Volatile Products and Unexpected High Formaldehyde Yield from the Atmospheric Oxidation of Methylsiloxanes, Environ. Sci. Technol., 54, 7136-7145, https://doi.org/10.1021/acs.est.0c01090, 2020.

Hay, P. J. and Wadt, W. R.: Ab initio effective core potentials for molecular calculations. Potentials for K to Au including the outermost core orbitals, J. Chem. Phys., 82, 299-310, https://doi.org/10.1063/1.448975, 1985a.

Hay, P. J. and Wadt, W. R.: Ab initio effective core potentials for molecular

calculations. Potentials for the transition metal atoms Sc to Hg., J. Chem. Phys., 82, 270-283, https://doi.org/10.1063/1.448799, 1985b.

Humphrey, W., Dalke, A., and Schulten, K.: VMD: Visual molecular dynamics, J Mol Graph Model, 14, 33-38, https://doi.org/10.1016/0263-7855(96)00018-5, 1996.

Kästner, J.: Umbrella sampling, Wires Comput Mol Sci, 1, 932-942, https://doi.org/10.1002/wcms.66, 2011.

Qu, R., Li, C., Liu, J., Xiao, R., Pan, X., Zeng, X., Wang, Z., and Wu, J.: Hydroxyl Radical Based Photocatalytic Degradation of Halogenated Organic Contaminants and Paraffin on Silica Gel, Environ. Sci. Technol., 52, 7220-7229, https://doi.org/10.1021/acs.est.8b00499, 2018.

Roy, L. E., Hay, P. J., and Martin, R. L.: Revised Basis Sets for the LANL Effective Core Potentials, J. Chem. Theory Comput., 4, 1029-1031, https://doi.org/10.1021/ct8000409, 2008.

Wadt, W. R. and Hay, P. J.: Ab initio effective core potentials for molecular calculations. Potentials for main group elements Na to Bi, J. Chem. Phys., 82, 282-298, https://doi.org/10.1063/1.448800, 1985.

Wang, X., Wei, Y., Zhang, H., Bao, L., He, M., and Yuan, S.: Understanding the properties of methyl vinyl ketone and methacrolein at the air-water interface: Adsorption, heterogeneous reaction and environmental impact analysis, Chemosphere, 283, 131183, https://doi.org/10.1016/j.chemosphere.2021.131183, 2021a.

Wang, X., Liu, S., Bao, L., Zhang, H., Yuan, S., He, M., and Yuan, S.: Enhanced uptake of methacrolein at the acidic nanoparticle interface: Adsorption, heterogeneous reaction and impact for the secondary organic aerosol formation, Sci Total Environ, 800, 149532, https://doi.org/10.1016/j.scitotenv.2021.149532, 2021b.

Yan, Z. and Truhlar, D. G.: The M06 suite of density functionals for main group thermochemistry, thermochemical kinetics, noncovalent interactions, excited states, and transition elements: Two new functionals and systematic testing of four M06 functionals and 12 other functionals (Th,

https://doi.org/10.1007/s00214-007-0310-x, 2015.

Zhao, Y. and Truhlar, D. G.: The M06 suite of density functionals for main group thermochemistry, thermochemical kinetics, noncovalent interactions, excited states, and transition elements: two new functionals and systematic testing of four M06-class functionals and 12 other functionals, Theor. Chem. Acc., 120, 215-241, https://doi.org/10.1007/s00214-007-0310-x, 2008a.

Zhao, Y. and Truhlar, D. G.: The M06 suite of density functionals for main group thermochemistry, thermochemical kinetics, noncovalent interactions, excited states, and transition elements: two new functionals and systematic testing of four M06 functionals and 12 other functionals, Theor. Chem. Acc., 119, 525-525, https://doi.org/10.1007/s00214-007-0401-8, 2008b.